

Published in final edited form as:

ACS Chem Biol. 2012 November 16; 7(11): 1796–1801. doi:10.1021/cb300193f.

Synthetic Allergen Design Reveals The Significance of Moderate Affinity Epitopes in Mast Cell Degranulation

Michael W. Handlogten¹, Tanyel Kiziltepe^{1,3}, Nathan J. Alves¹, and Basar Bilgicer^{1,2,3,*}

¹Department of Chemical and Biomolecular Engineering, University of Notre Dame, Notre Dame IN 46556

²Department of Chemistry and Biochemistry, University of Notre Dame, Notre Dame IN 46556

³Advanced Diagnostics and Therapeutics, University of Notre Dame, Notre Dame IN 46556

Abstract

This study describes the design of a well-defined homotetravalent synthetic allergen (HTA) system to investigate the effect of hapten-IgE interactions on mast cell degranulation. A library of DNP-variants with varying affinities for IgE^{DNP} was generated (K_{ds} 8.1 nM – 9.2 μM), and 8 HTAs spanning this range were synthesized via conjugation of each DNP-variant to the tetravalent scaffold. HTAs with hapten $K_{ds} < 235$ nM stimulated degranulation following a bell-shaped dose response curve with maximum response occurring near the hapten K_d . HTAs with hapten K_{ds} 235 nM failed to stimulate degranulation. To mimic physiological conditions, the percent of allergen specific IgE on cell surface was varied, and maximum degranulation occurred at 25% IgE^{DNP}. These results demonstrated that moderate hapten-IgE affinities are sufficient to trigger mast cell degranulation. Moreover, this study established the HTA design as a well-defined, controllable, and physiologically relevant experimental system to elucidate the mast cell degranulation mechanism.

Type-I hypersensitive reactions (allergies) result from the crosslinking of IgE antibodies that are bound to their high-affinity receptor (FcεRI) on the surface of mast cells by multivalent allergens.¹ The allergen-IgE interactions on the mast cell surface initiate a complex series of downstream signaling cascades, including phosphorylation of the immunoreceptor tyrosine-based activation motifs (ITAMs) in the β- and γ- chains of FcεRI, resulting in mast cell degranulation.^{2, 3}

In allergy research, the most widely used experimental model utilizes the rat basophilic leukemia cell (RBL) / dinitrophenyl (DNP) system, where the RBL cells are primed with monoclonal IgE^{DNP} (DNP-specific IgE) antibodies.⁴ The IgE^{DNP} presenting RBL cells are then stimulated with a multivalent synthetic allergen, which is typically synthesized by conjugating multiple DNP moieties to scaffolds such as BSA, OVA, or nanoparticles, to induce a degranulation response.^{3, 5–8} Although this experimental system has helped elucidate critical aspects of mast cell degranulation, it has several limitations. One common limitation is that in most previously performed assays that utilized the RBL/DNP system, only one type of IgE antibody/hapten pair, namely IgE^{DNP}/DNP, was used. In physiological

*Corresponding Author bbilgicer@nd.edu.

Associated Content

Supporting Information

DLS of HTA/IgE^{DNP} with discussion of complex formation. This material is available free of charge via the internet at <http://pubs.acs.org>.

The authors declare no competing financial interest.

systems, multiple IgE antibodies are produced that bind with a wide range of affinities to various epitopes present on the allergen, providing for a polyclonal response.⁹ Indeed, the level of a particular IgE that is specific for a given allergen ranges from 0.1% to 20% of all IgEs present in an allergy patient's serum.⁶ As a result of this variability, mast cells in physiological systems present multiple clones of IgEs specific for an array of allergens with varying affinities.¹⁰ Therefore, experimental systems where mast cells are primed exclusively with IgE^{DNP} provide an unrealistic representation of physiological systems. Furthermore, DNP binds to IgE^{DNP} with an atypically high monovalent affinity, which does not represent the range of IgE affinities for allergy epitopes in nature.^{9, 11} Finally, the commonly studied synthetic allergens, which were synthesized by non-specific conjugation of DNP to scaffolds such as BSA, are poorly defined. The chemical conjugation methods used often result in significant heterogeneity in the number of haptens per scaffold, which can range between 2 to 25 haptens per allergen in contrast to natural allergens which typically have 1 to 5 immunodominant epitopes.^{3, 5, 6, 8, 10, 14-17} Further complications arise as only the average number of haptens per synthetic allergen can be determined, many haptens in these scaffolds may not be available to bind to IgE-FcεRI complexes on cell surface due to steric constraints, and these poorly defined allergens likely have multiple geometries of engagement with surface bound IgE complicating conclusions drawn from studies using these allergens.^{12, 13} It is well known that the structure of an antigen is crucial for its activity particularly when designing multivalent ligands to bind to cell surface receptors.¹⁸⁻²⁰ In an attempt to clarify the properties of allergens, a few reports used molecularly uniform synthetic allergens and were able to identify the minimum number of haptens needed to stimulate a cellular response.²¹⁻²³ However, the experimental systems used in these studies still did not address the question of the effect of monovalent hapten affinity on mast cell activation, and utilized only a single IgE/hapten pair. With the limitations of the previously used allergy models in mind, there is a clear need for an improved experimental system to study allergic responses, which will allow controlled variability in the monovalent hapten affinity and valency on a well-defined scaffold, as well as the ratio of allergen-specific IgE on the surface, for a more complete elucidation of the mechanism of mast cell degranulation.

In this study, we improved the classic RBL/DNP model by designing a homotetravalent synthetic allergen (HTA), which provides complete control over the conjugated hapten moieties and better represents the number of immunodominant epitopes on natural allergens. A tetravalent scaffold was chosen for the synthetic allergen for several reasons. First, we wanted to model the number of immunodominant epitopes found in natural systems, which typically range from 1 to 5.^{10, 14-17} A tetravalent system is particularly suitable to mimic some common allergens such as Ara h 3 of peanut and Tri a 14 of wheat, which have four immunodominant epitopes.^{24, 25} Second, literature reports describe that potent degranulation is achieved by synthetic allergens with a valency of 3 or higher.^{22, 23} Finally, each hapten in the design should be available for binding to IgE antibodies simultaneously without steric constraints, and a valency of 5 or higher would cause such constraints. Furthermore, a tetravalent design was amenable to Fmoc chemistry on a solid support allowing for the rapid synthesis and purification of the synthetic allergens as described in the methods section. To address the effect of monovalent hapten affinity on mast cell activation, we synthesized DNP variants, each with a different affinity for IgE^{DNP}, generating new IgE^{DNP}/hapten pairs with a range of monovalent affinities. This was accomplished by conjugating DNP to various amino acids. It has been previously demonstrated that DNP-amino acids have a wide range in affinity for IgE^{DNP} depending on the amino acid the hapten DNP is conjugated to.¹¹ The differences in the affinity of the DNP-amino acids are due to the properties of the side chains of the amino acids. Specifically, we synthesized the 12 DNP variants listed in Figure 1 and determined the affinity of each molecule to IgE^{DNP} using a fluorescence

quenching method described in our earlier publication.⁸ Our results demonstrated that the affinity of the DNP variants for IgE^{DNP} ranged from $K_d = 8.1$ nM to 9.2 μ M (Figure 2).

From the 12 analyzed DNP variants, we selected 8 representative haptens that spanned the range of affinities, and synthesized the respective HTAs by conjugating each variant to the tetravalent scaffold shown in Figure 3. The tetravalent scaffold connects each hapten moiety to the core of the molecule using 8 units of ethylene glycol to provide enough length to ensure that all four haptens are available to bind to IgE^{DNP}.^{26,27} Also, glutamic acid residues were incorporated into the scaffold to provide a means of conjugating each moiety to the ethylene glycol linker as well as provide a charge to increase the solubility of the synthetic allergens. The extended length of each ethylene glycol linker is 3.2 nm providing a maximum separation of 6.4 nm between haptens. The flexibility and solubility of the HTA design ensures that each hapten is available to bind to IgE^{DNP}, yet the length of the ethylene glycol linker makes it sterically unfavorable for a single IgE to bind to two haptens on a single HTA.^{28–30} To ensure that the HTAs were capable of simultaneously binding to multiple IgEs, the size of IgE/HTA complexes were measured using dynamic light scattering (DLS). The size of monomeric IgE^{DNP} was measured to be 10.7 nm. Upon the addition of a stoichiometric amount of HTA (HTA:IgE, 1:2), the peak at 10.7 nm disappeared and a new peak at ~20 nm appeared indicating the formation of IgE/HTA complexes. These complexes formed in less than a minute and were stable over several hours suggesting that thermodynamic equilibrium was reached. DLS measurements of IgE^{DNP} resulted in a similar ~20 nm particle size with all 8 HTA molecules (Figure S1B). Since, the design of HTA prevents bivalent binding to a single antibody, (when mixed at stoichiometric ratio of haptens to binding sites) the only possible complex that can form with a diameter of 20 nm is a bicyclic antibody tetramer (IgE₄HTA₂); see supporting information for further discussion on the complex formation. These results indicated that HTAs were able to simultaneously bind tetravalently to and form complexes with IgE^{DNP} antibodies. Specifically, the DLS result indicates that each of the four haptens on a single HTA molecule were able to bind to a different IgE Fab domain, and therefore, the HTA is indeed acting as a tetravalent molecule in solution. As a result, we predicted that there would not be any steric issues preventing HTA from effectively presenting all four haptens for binding and crosslinking IgE antibodies on mast cell surfaces.

Next, we studied the effect of monovalent hapten affinity on mast cell degranulation by using the synthesized HTAs. Each of the HTAs were assayed with RBL cells that were primed with a saturating concentration of IgE^{DNP} to ensure that all FcεRI receptors were associated with an IgE. The five tightest binding HTAs synthesized from haptens with monovalent affinities ranging between $K_d = 8.1$ – 105 nM for IgE^{DNP} were all determined to be potent stimulators of degranulation (Figure 4A). Conversely, the three HTAs synthesized from haptens with monovalent affinities ranging between $K_d = 235$ nM – 6.5 μ M failed to stimulate a degranulation response.³¹ All five HTAs that stimulated degranulation demonstrated a bell shaped response curve – where degranulation first increased, reached a maximum, and then decreased with increasing HTA concentration. Importantly, the potency of the HTAs both in terms of the concentration of HTA required to stimulate a response and the intensity of the degranulation response correlated with the monovalent hapten affinity. Interestingly, the concentration at which each HTA triggered its maximum response was in the range of the monovalent K_d of the hapten used in the HTA. This observation suggests that although HTAs are multivalent, an avidity enhancement due to multivalent binding to surface bound IgE does not take place. This is an expected result given that the average IgE distance on the cell surface is ~50 nm; much larger than the distance the HTA can span and it has been previously shown that for significant enhancement in avidity the receptors and ligands must be equally spaced.^{32–34} Therefore, we predict that the HTA molecule first binds to a single IgE-FcεRI complex, and then diffuses across the surface to bind to another

IgE-FcεRI complex until signaling competent clusters are formed. In the case of weaker binding HTAs (monovalent $K_d = 235$ nM), it is likely that the rate of dissociation of the hapten with IgE^{DNP} is too rapid to form signaling competent clusters of IgE-FcεRI on the mast cells.

In physiological systems, there are multiple clones of IgEs in the serum and the level of a particular IgE that is specific for a given allergen ranges from 0.1% to 20% of all serum IgEs. Therefore, mast cells present multiple clones of IgEs on their surface with each particular clone of IgE occupying only a certain fraction of the total FcεRI receptors. To mimic physiologically relevant conditions, we assayed the HTAs for their efficiency in RBL degranulation, when the surface bound IgE^{DNP} decreased from 100% to 25% (Figure S2), while keeping the total IgE concentration constant at saturating levels by using IgE^{dansyl} as the orthogonal IgE.³⁵ Surprisingly, when the percentage of IgE^{DNP} on the surface of mast cells was decreased to 25%, the intensity of the degranulation response increased for all five HTAs with a monovalent K_d between 8.1 – 105 nM (Figure 4B). While the maximum degranulation response increased ~2.2 fold from 40% to 90% for the three tightest binding HTAs ($K_d = 8.1 - 21$ nM), the response increased ~2.8 fold from 20% to 55% for the HTAs with intermediate monovalent affinities ($K_d = 73 - 105$ nM). Indeed, the least potent HTA [DNP-Lys], which induced only a moderate response (20%) when 100% IgE^{DNP} was used, induced a much stronger response (55%) when IgE^{DNP} was reduced to 25%. This exceeded the maximum response observed with 100% IgE, even when compared to the strongest stimulator – HTA [DNP-Thr] (38%). In all experiments, the concentration where the maximum degranulation response was achieved remained unaffected with the change in the percent of IgE^{DNP} present on the cell surface. We did not observe any degranulation response with the three weakest binding HTAs ($K_d = 235 - 6.5$ μM) under any circumstances. A more thorough study of the effect of the ratio of allergen specific IgE to orthogonal IgE on mast cell degranulation was performed by modifying surface IgE^{DNP} from 100% to 0%. As the percent of IgE^{DNP} on the surface of mast cells decreased, the degranulation response of the RBL cells initially increased and then rapidly dropped off (Figure 4C). This bell shaped curve revealed that maximum degranulation was achieved with the RBL cells that were primed with only ~25% IgE^{DNP}. While these results were surprising, they were not completely unexpected. Natural allergy systems are capable of strong responses (anaphylaxis) which occur with mast cells primed with 20% or less allergen specific IgE.⁶ Furthermore, it has been demonstrated that maximal degranulation can occur with only 5% IgE cross-linking on mast cell surface.³⁶ Additionally, an inverse correlation has been shown between FcεRI aggregate size and degranulation response. Studies demonstrated that formation of small aggregates triggered robust degranulation, while large aggregates promoted receptor internalization and was associated with decreased degranulation.^{3, 37} It is likely that as the percent of allergen specific IgE decreased on the mast cell surface, the size of the HTA-induced FcεRI aggregates decreased, thereby forming signaling competent clusters that triggered enhanced degranulation.

In conclusion, the HTAs developed in this study provide a well-defined experimental system that allows controlled variability in the monovalent hapten affinity, as well as the ratio of allergen-specific IgE on the cell surface for a more complete elucidation of the mechanism of mast cell degranulation. Studying the effect of hapten affinity in mast cell degranulation has traditionally been challenging due to the limited availability of hapten/IgE pairs as research tools. We addressed this problem by taking a chemical biology approach where we generated 12 hapten molecules for IgE^{DNP} to span a broad range of affinities (K_d s from 8.1 nM to 9.2 μM), and synthesized well characterized synthetic allergens by conjugating these haptens to the HTA scaffold. Importantly, the exact valency of the HTA scaffold enabled studying the effect of affinity on mast cell degranulation without other compounding factors. This type of analysis would not have been possible with the previously used synthetic

allergens that were generated by conjugating haptens to a protein scaffolds, as these scaffolds yield a high heterogeneity in the hapten valency per scaffold. Our results obtained with the HTA system demonstrated that IgE antibodies do not necessarily need to have a high affinity for allergy epitopes to trigger mast cell degranulation; rather the affinity range is in fact quite broad. In addition, our results suggest that there may be a threshold hapten affinity ($K_d = \sim 105$ nM) below which mast cell degranulation is not triggered. Our studies also established that the maximal degranulation consistently occurred at allergen concentrations close to the K_d value of the hapten-IgE interaction. Surprisingly, we found that maximum degranulation occurred when the mast cells presented only 25% allergen specific IgE. This result indicates that there is an optimal amount of FcεRI crosslinking to initiate degranulation above or below which the intensity of the response decreases. This finding challenges the existing paradigms and raises new important questions on the mechanism of mast cell degranulation, emphasizing the significance of physiologically relevant experimental model systems, such as HTA, in allergy research. Such studies were not possible with the previously established models demonstrating the HTA design as a well-defined, physiologically relevant, and controllable experimental system to address several critical issues in mast cell degranulation. We believe the introduction of the HTA model system as a new research tool will significantly benefit mast cell degranulation and allergy research.

Materials and Methods

Materials

N-Fmoc-amido-dPEG₈-acid from Quanta BioDesign, *N*-Fmoc-amino acids, NovaPEG Rink Amide resin, and 2-(1H-Benzotriazole-1-yl)-1,1,3,3-tetramethyluronium hexafluorophosphate (HBTU) were purchased from EMD Biosciences. 1-Fluoro-2,4-dinitrobenzene (DNP), *N,N*-diisopropylethylamine (DIEA), trifluoroacetic acid (TFA), and piperidine from Sigma and *N,N*-dimethylformamide (DMF) (>99.8%) were purchased from Thermo Fisher. IgE^{dansyl} (clone 27-74) was purchased from BD Bioscience, and IgE^{DNP} (clone SPE-7) was purchased from Sigma.

Synthesis of Monovalent Haptens and Homotetravalent Allergens

All molecules were synthesized using standard Fmoc chemistry on solid support. Fmoc protected amino acids were activated with HBTU and DIEA in DMF for 3 minutes and coupling was monitored with Keiser test. Fmoc protection group was removed by three applications of 3 minute exposure to 20% piperidine in DMF. Branching for the HTAs was achieved using the lysine derivate Fmoc-Lys(Fmoc)-OH. Upon treatment with piperidine both Fmoc groups were removed providing two amine groups (terminal amine and the sidechain ε-amine). Next, Fmoc-Lys(Fmoc)-OH was added to each of the newly generated free amines followed by the removal of the fmoc protecting group. This resulted in 4 primary amine groups for the conjugation of the DNP haptens. The synthesized ligands were cleaved from the solid support using 2 × 94/3/3 TFA/H₂O/TIS for 30 minutes. All molecules were purified using RP-HPLC on an Agilent 1200 series system with a semi-preparative Zorbax C18 column (9.4mm × 250mm), using linear gradient of 2.5% min⁻¹ increments in acetonitrile content with a 4.0 mL/min flow rate. The column eluent was monitored with a diode array detector allowing a spectrum from 200 to 400 nm to be analyzed. The purified products were characterized using a Bruker micrOTOF II mass spectrometer in negative ion mode with the exception of DNP-Lys and HTA[DNP-Lys] which were analyzed in positive ion mode. The purity of all synthesized ligands was estimated to be >97% by an analytical injection using the above described HPLC with a Zorbax C18 analytical column (4.6mm × 150mm). The calculated exact mass of DNP-Thr (C₁₅H₁₉N₅O₉) was 413.1183 Da; found 412.1318 Da, the calculated exact mass of DNP-Glu (C₁₁H₁₂N₄O₇) was 312.0706 Da; found

311.0773 Da, the calculated exact mass of DNP₂-His (C₂₃H₂₂N₁₀O₁₂) was 615.1310 Da; found 614.1429 Da, the calculated exact mass of DNP-Nor (C₁₇H₂₃N₅O₈) was 425.1547 Da; found 424.1660 Da, the calculated exact mass of DNP₂-Tyr (C₂₆H₂₃N₇O₁₃) was 641.1354 Da; found 640.1433 Da, the calculated exact mass of DNP-Trp (C₂₂H₂₂N₆O₈) was 498.1499 Da; found 497.1587 Da, the calculated exact mass of DNP-Lys (C₁₂H₁₇N₅O₅) was 311.1230 Da; found 312.1297 Da, the calculated exact mass of TNT-Glu (C₁₁H₁₁N₅O₉) was 357.0557 Da; found 356.0733 Da, the calculated exact mass of DNP-Asn (C₁₅H₁₈N₆O₉) was 426.1135 Da; found 425.1095 Da, the calculated exact mass of DNP-Sar (C₁₄H₁₇N₅O₈) was 383.1077 Da; found 382.1161 Da, the calculated exact mass of DNP-Pro (C₁₆H₁₉N₅O₈) was 409.1234 Da; found 408.1306 Da, the calculated exact mass of Phe(4-NO₂) (C₁₆H₂₀N₄O₇) was 380.1332 Da; found 379.1436 Da, the calculated exact mass of HTA[DNP-Thr] (C₁₆₅H₂₇₀N₃₀O₇₉) was 3935.8032 Da; found 3934.9095 Da, the calculated exact mass of HTA[DNP-Glu] (C₁₄₉H₂₄₂N₂₆O₇₁) was 3531.6125 Da; found 3530.6816 Da, the calculated exact mass of HTA[DNP₂-His] (C₁₉₇H₂₇₈N₄₆O₉₁) was 4743.8540 Da; found 4742.9757 Da, the calculated exact mass of HTA[DNP₂-Tyr] (C₂₀₉H₂₈₆N₃₈O₉₅) was 4847.8717 Da; found 4846.8032 Da, the calculated exact mass of HTA[DNP-Lys] (C₁₅₄H₂₆₇N₃₁O₆₁) was 3526.8744 Da; found 3527.9637 Da, the calculated exact mass of HTA[TNT-Glu] (C₁₄₉H₂₃₈N₃₀O₇₀) was 3711.5528 Da; found 3710.6342 Da, the calculated exact mass of HTA[DNP-Sar] (C₁₆₁H₂₆₂N₃₀O₇₅) was 3585.7610 Da; found 3814.8076 Da, the calculated exact mass of HTA[DNP-Pro] (C₁₆₉H₂₇₀N₃₀O₇₅) was 3919.8236 Da; found 3918.8382 Da.

Fluorescence Quenching Assay

The binding constants of the monovalent haptens to IgE^{DNP} were determined as previously described.⁸ Briefly, DNP quenches the fluorescence from the IgE tryptophan residues, occurring at 335 nm, only when the two molecules are in proximity to each other (~10 nm). The monovalent haptens were titrated into a 96 well plate containing 200 μ L solution of 10 nM IgE^{DNP} in PBS. All experiments were done in at least triplicates.

RBL Degranulation Assay

RBL cells were kindly provided by Dr. Wilson (University of New Mexico). RBL cells were maintained as described previously.³⁸ For the degranulation assay, cells were plated at 0.5×10^6 cells/mL in a 96 well plate and were incubated overnight. The next morning, 1 μ g/mL IgE was introduced to prime the cells at saturating concentrations. Unbound IgE was washed away immediately before experiments and indicated concentrations of each of the HTAs were introduced into the wells. RBL degranulation was detected spectroscopically by measuring the activity of the secreted β -hexosaminidase by using the substrate p-nitrophenyl-N-acetyl- β -O-glucosamine (pNAG). Triton X (1%) was used to lyse the cells and release the contents of the granules. All degranulation experiments were normalized to the Triton X signal. All cellular degranulation assays were performed in at least triplicates.

IgE^{DNP}/HTA Complex Formation

The sizes of cyclic IgE^{DNP} complexes that formed upon addition of HTA were measured using a Malvern Zetasizer Nano S. To measure the size of IgE^{DNP}, 0.8 μ M IgE^{DNP} was prepared in PBS and the particle size was measured. To measure IgE^{DNP}/HTA complex formation, a stoichiometric amount of each HTA (0.4 μ M) was mixed with 0.8 μ M IgE^{DNP} and the complex size was measured using an estimated refractive index of 1.45.

Supplementary Material

Refer to Web version on PubMed Central for supplementary material.

Acknowledgments

This research is supported by NIH-NIAID R03 AI085485.

References

1. Metzger H. Transmembrane signaling - the joy of aggregation. *J. Immunol.* 1992; 149:1477–1487. [PubMed: 1324276]
2. Blank U, Rivera J. Assays for regulated exocytosis of mast cell granules. *Curr Protoc Cell Biol.* Chapter 15. 2006 Unit 15.11.
3. Andrews NL, Pfeiffer JR, Martinez AM, Haaland DM, Davis RW, Kawakami T, Oliver JM, Wilson BS, Lidke DS. Small, mobile Fc Epsilon R1 receptor aggregates are signaling competent. *Immunity.* 2009; 31:469–479. [PubMed: 19747859]
4. Passante E, Frankish N. The RBL-2H3 cell line: its provenance and suitability as a model for the mast cell. *Inflammation Res.* 2009; 58:737–745.
5. Collins AM, Basil M, Nguyen K, Thelian D. Rat basophil leukaemia (RBL) cells sensitized with low affinity IgE respond to high valency antigen. *Clinical and Experimental Allergy.* 1996; 26:964–970. [PubMed: 8877164]
6. Collins AM, Thelian D, Basil M. Antigen valency as a determinant of the responsiveness of IgE-sensitized rat basophil leukemia-cells. *Int. Arch. Allergy Immunol.* 1995; 107:547–556. [PubMed: 7620369]
7. Huang Y, Liu H, Xiong X, Chen Y, Tan W. Nanoparticle-mediated IgE-receptor aggregation and signaling in RBL mast cells. *J. Am. Chem. Soc.* 2009; 131:17328–17334. [PubMed: 19929020]
8. Handlogten MW, Kiziltepe T, Moustakas DT, Bilgicer B. Design of a heterobivalent ligand to inhibit IgE clustering on mast cells. *Chem. Biol.* 2011; 18:1179–1188. [PubMed: 21944756]
9. Wang J, Lin J, Bardina L, Goldis M, Nowak-Wegrzyn A, Shreffler WG, Sampson HA. Correlation of IgE/IgG4 milk epitopes and affinity of milk-specific IgE antibodies with different phenotypes of clinical milk allergy. *J. Allergy Clin. Immunol.* 2010; 125:695–702. [PubMed: 20226304]
10. Cerecedo I, Zamora J, Shreffler WG, Lin J, Bardina L, Dieguez MC, Wang J, Muriel A, de la Hoz B, Sampson HA. Mapping of the IgE and IgG4 sequential epitopes of milk allergens with a peptide microarray-based immunoassay. *J. Allergy Clin. Immunol.* 2008; 122:589–594. [PubMed: 18774394]
11. James LC, Tawfik DS. The specificity of cross-reactivity: promiscuous antibody binding involves specific hydrogen bonds rather than nonspecific hydrophobic stickiness. *Protein Science.* 2003; 12:2183–2193. [PubMed: 14500876]
12. Xu KL, Goldstein B, Holowka D, Baird B. Kinetics of multivalent antigen DNP-BSA binding to IgE-Fc Epsilon RI in relationship to the stimulated tyrosine phosphorylation of Fc Epsilon RI. *J. Immunol.* 1998; 160:3225–3235. [PubMed: 9531278]
13. Hlavacek W, Posner R, Perelson A. Steric effects on multivalent ligand-receptor binding: exclusion of ligand sites by bound cell surface receptors. *Biophys. J.* 1999; 76:3031–3043. [PubMed: 10354429]
14. Pacios LF, Tordesillas L, Cuesta-Herranz J, Compes E, Sanchez-Monge R, Palacin A, Salcedo G, Diaz-Perales A. Mimotope mapping as a complementary strategy to define allergen IgE-epitopes: peach Pru p 3 allergen as a model. *Mol. Immunol.* 2008; 45:2269–2276. [PubMed: 18242709]
15. Rouge P, Culierrier R, Sabatiera V, Granier C, Rance F, Barre A. Mapping and conformational analysis of IgE-binding epitopic regions on the molecular surface of the major Ara h 3 legumin allergen of peanut (*Arachis Hypogaea*). *Mol. Immunol.* 2009; 46:1067–1075. [PubMed: 18995911]
16. Christensen LH, Holm J, Lund G, Riise E, Lund K. Several distinct properties of the IgE repertoire determine effector cell degranulation in response to allergen challenge. *J. Allergy Clin. Immunol.* 2008; 122:298–304. [PubMed: 18572230]
17. Tanabe S. Epitope peptides and immunotherapy. *Curr. Protein Peptide Sci.* 2007; 8:109–118. [PubMed: 17305564]

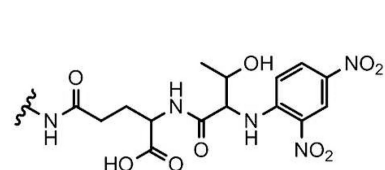
18. Kiessling LL, Gestwicki JE, Strong LE. Synthetic multivalent ligands as probes of signal transduction. *Angew. Chem., Int. Ed.* 2006; 45:2348–2368.
19. Puffer EB, Pontrello JK, Hollenbeck JJ, Kink JA, Kiessling LL. Activating B cell signaling with defined multivalent ligands. *ACS Chem. Biol.* 2007; 2:252–262. [PubMed: 17432821]
20. Mammen M, Choi S-k, Whitesides GM. Polyvalent interactions in biological systems: implications for design and use of multivalent ligands and inhibitors. *Angew. Chem., Int. Ed.* 1998; 37:2754–2794.
21. Posner RG, Subramanian K, Goldstein B, Thomas J, Feder T, Holowka D, Baird B. Simultaneous cross-linking by two nontriggering bivalent ligands causes synergistic signaling of IgE RceR1 complexes. *J. Immunol.* 1995; 155:3601–3609. [PubMed: 7561059]
22. Posner RG, Geng D, Haymore S, Bogert J, Pecht I, Licht A, Savage PB. Trivalent antigens for degranulation of mast cells. *Org. Lett.* 2007; 9:3551–3554. [PubMed: 17691795]
23. Sil D, Lee JB, Luo D, Holowka D, Baird B. Trivalent ligands with rigid DNA spacers reveal structural requirements for IgE receptor signaling in RBL mast cells. *ACS Chem. Biol.* 2007; 2:674–684. [PubMed: 18041817]
24. Rabjohn P, Helm E, Stanley J, West C, Sampson H, Burks A, Bannon G. Molecular cloning and epitope analysis of the peanut allergen Ara h 3. *J. Clin. Invest.* 1999; 103:535–542. [PubMed: 10021462]
25. Denery-Papini S, Bodinier M, Pineau F, Triballeau S, Tranquet O, Adel-Patient K, Moneret-Vautrin DA, Bakan B, Marion D, Mothes T, Mameri H, Kasarda D. Immunoglobulin-E-binding epitopes of wheat allergens in patients with food allergy to wheat and in mice experimentally sensitized to wheat proteins. *Clinical and Experimental Allergy.* 2011; 41:1478–1492. [PubMed: 21771117]
26. Bilgicer B, Moustakas DT, Whitesides GM. A Synthetic trivalent hapten that aggregates anti-2,4-DNP IgG into bicyclic trimers. *J. Am. Chem. Soc.* 2007; 129:3722–3728. [PubMed: 17326636]
27. Stefanick JF, Kiziltepe T, Handlogten MW, Alves NJ, Bilgicer B. Enhancement of antibody selectivity via bicyclic complex formation. *Journal of Physical Chemistry Letters.* 2012; 3:598–602.
28. Roux KH, Strelets L, Brekke OH, Sandlie I, Michaelsen TE. Comparisons of the ability of human IgG3 hinge mutants, IgM, IgE, and IgA2, to form small immune complexes: a role for flexibility and geometry. *J. Immunol.* 1998; 161:4083–4090. [PubMed: 9780179]
29. Strelets L, Roux KH, Brekke OH, Sandlie I, Michaelsen T. The role of the hinge region in human IgG immune complex formation. *FASEB J.* 1996; 10:973–973.
30. Baird EJ, Holowka D, Coates GW, Baird B. Highly effective poly(ethylene glycol) architectures for specific inhibition of immune receptor activation. *Biochemistry.* 2003; 42:12739–12748. [PubMed: 14596588]
31. This was Tested Up to 50 μM ; Results Not shown Beyond 1 μM .
32. Calculated using a diameter of 10 μm for RBL cells and $\sim 300,000$ FceRI receptors per cell, while assuming homogenous surface distribution of the receptors.
33. Posner RG, Savage PB, Peters AS, Macias A, DelGado J, Zwartz G, Sklar LA, Hlavacek WS. A quantitative approach for studying IgE-Fc Epsilon RI aggregation. *Mol. Immunol.* 2002; 38:1221–1228. [PubMed: 12217387]
34. Rai P, Padala C, Poon V, Saraph A, Basha S, Kate S, Tao K, Mogridge J, Kane R. Statistical pattern matching facilitates the design of polyvalent inhibitors of anthrax and cholera toxins. *Nat. Biotechnol.* 2006; 24:582–586. [PubMed: 16633350]
35. IgE that is not specific to DNP; none of the DNP variants bind up to 100 μM to IgE^{Dansyl}, (Data Not shown).
36. Ortega E, Schweitzerstenner R, Pecht I. Possible orientational constraints determine secretory signals induced by aggregation of IgE receptors on mast-cells. *EMBO J.* 1988; 7:4101–4109. [PubMed: 2977332]
37. Seagrave J, Oliver JM. Antigen-dependent transition of IgE to a detergent-insoluble form is associated with reduced IgE receptor-dependent secretion from RBL-2H3 mast-cells. *J. Cell. Physiol.* 1990; 144:128–136. [PubMed: 2142164]

38. Andrews N, Lidke KA, Hsieh G, Wilson BS, Oliver JM, Lidke DS. High affinity IgE receptor diffusional dynamics measured by single quantum dot tracking in resting and activated cells. *FASEB J.* 2007; 21:A184–A184.

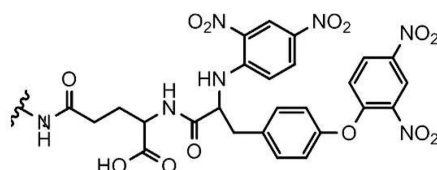
\$watermark-text

\$watermark-text

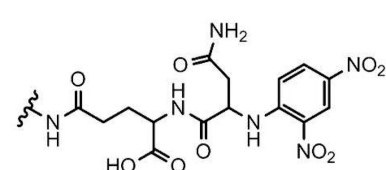
\$watermark-text



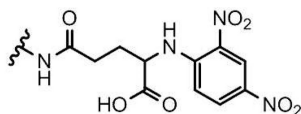
DNP-Thr $K_d = 8.1 \pm 0.6$ nM



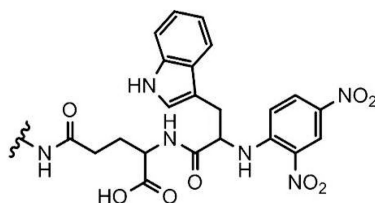
DNP₂-Tyr $K_d = 73 \pm 2$ nM



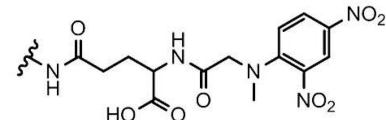
DNP-Asn $K_d = 340 \pm 40$ nM



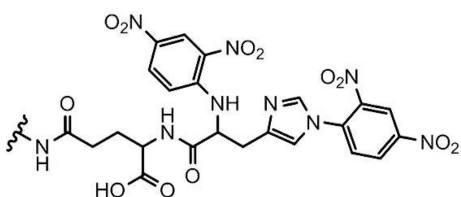
DNP-Glu $K_d = 15 \pm 2.5$ nM



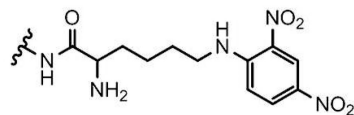
DNP-Trp $K_d = 95 \pm 14$ nM



DNP-Sar $K_d = 690 \pm 100$ nM



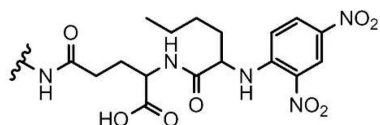
DNP₂-His $K_d = 21 \pm 5$ nM



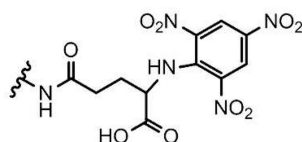
DNP-Lys $K_d = 105 \pm 15$ nM



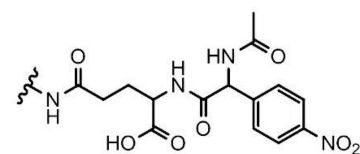
DNP-Pro $K_d = 6550 \pm 500$ nM



DNP-Nor $K_d = 22 \pm 5$ nM



TNT-Glu $K_d = 235 \pm 30$ nM



Phe(4-NO₂) $K_d = 9200 \pm 900$ nM

Figure 1.

DNP hapten variants and their monovalent binding affinities to IgE^{DNP}. The indicated amide nitrogens provide functionality for conjugation to the HTA scaffold.

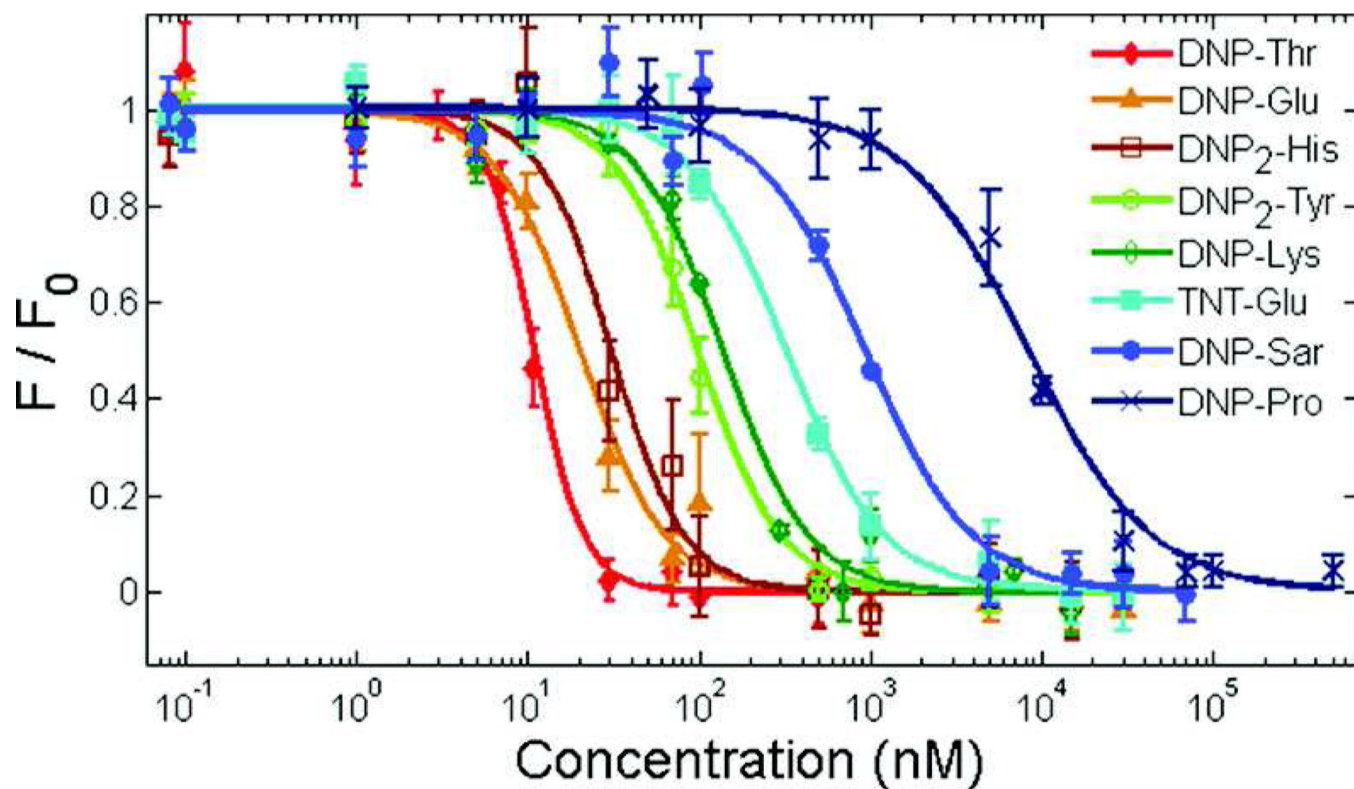


Figure 2. Representative binding curves of DNP hapten variants to IgE^{DNP}. Binding was detected from the fluorescence quenching of IgE^{DNP} tryptophan residues by DNP. Data represents means \pm SD.

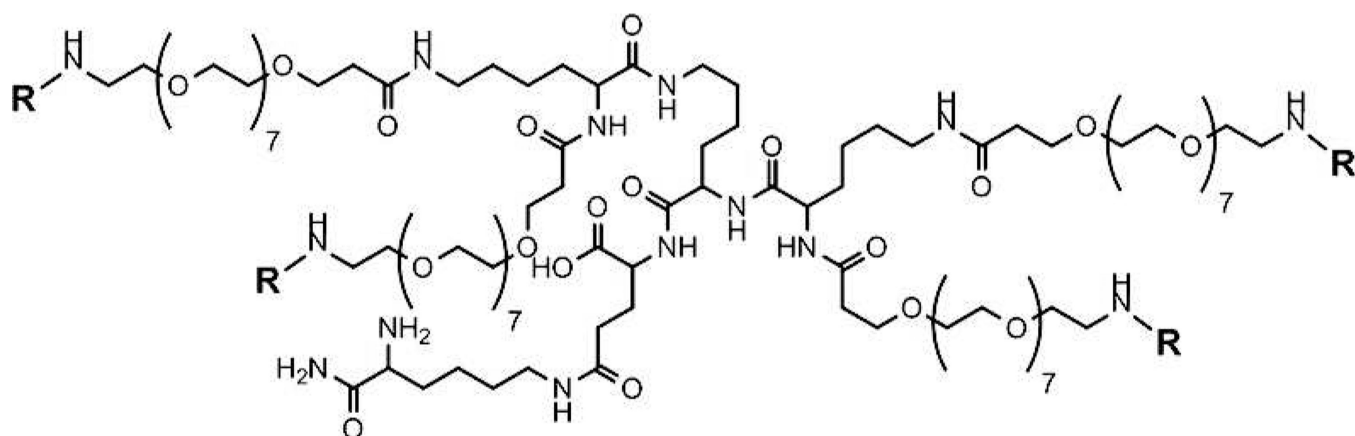


Figure 3. The HTA scaffold is shown. The R groups denote one of the DNP variants for each HTA.

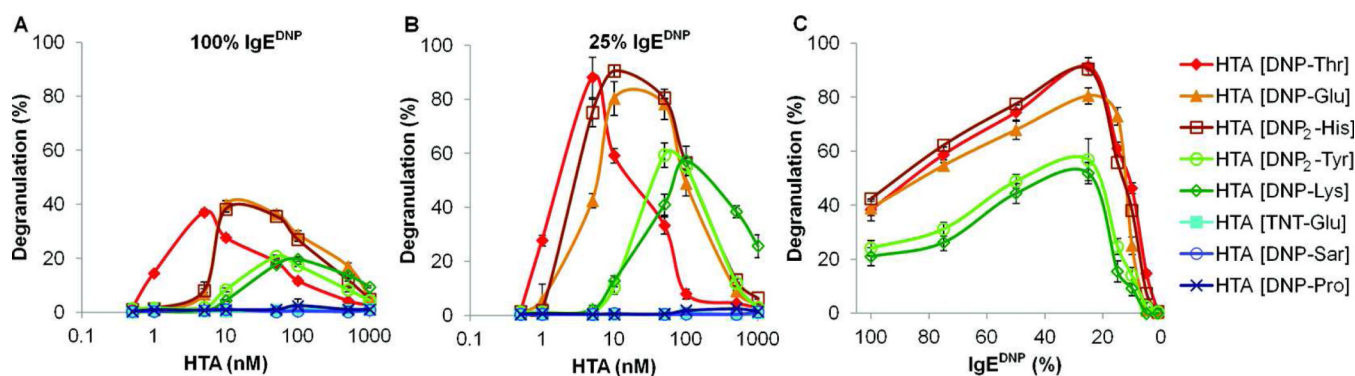


Figure 4.

Mast cell degranulation response to stimulation by HTAs. The mast cells were primed with 100% IgE^{DNP} in (A), and 25% IgE^{DNP} and 75% orthogonal IgE (IgE^{dansyl}) in (B), then exposed to one of the eight HTAs at the indicated concentrations. The potency, both in terms of concentration required to stimulate the maximum response as well as the overall strength of degranulation response, directly correlated with the monovalent hapten affinity. (C) The effect of hapten specific IgE (IgE^{DNP}) percent for achieving maximum degranulation response was investigated. The maximum response for all HTAs was observed for RBL cells primed with 25% IgE^{DNP}.